Weibull Statistical Analysis of Area and Volume Effects on the Breakdown Strength in Liquid Nitrogen

H. Goshima, N. Hayakawa, M. Hikita, H. Okubo

Nagoya University, Nagoya, Japan

and K. Uchida

Chubu Electric Power Co. Inc., Nagoya, Japan

ABSTRACT

In order to examine the area and the volume effects on breakdown strength in liquid nitrogen (LN_2), we measured dc and ac breakdown voltages in LN_2 with sphere to plane and coaxial cylindrical electrode configurations. We also carried out statistical analysis of the experimental results using the Weibull distribution and discussed with the statistical stressed electrode area (SSEA) and/or liquid volume (SSLV). The dc and ac breakdown strength in LN_2 decreased to 1/5 with increasing SSEA and SSLV over the wide range from 10^0 to 10^5 mm^2 and from 10^{-1} to 10^5 mm^3, respectively. Weibull shape parameter m for the sphere to plane and the coaxial cylindrical electrodes were estimated to be 6 to 8 and 11 to 13, respectively; the breakdown strength in LN_2 saturated with increasing SSEA and SSLV. From these results, it was verified that the area and the volume effects definitely determined the breakdown strength in LN_2. The results of the Weibull statistics were compared with the conventional concept of the stressed electrode area (SEA) and liquid volume (SLV). Consequently, SSEA or SSLV was found to be nearly equal to 80 to 85% of SEA or SLV.

1. INTRODUCTION

IT is necessary to establish the electrical insulation technique in liquid nitrogen (LN_2) in order to realize a high temperature superconducting electric power system [1–4]. However, most of the data on electrical breakdown in LN_2 have been obtained under limited experimental conditions. Thus, it is important to obtain data available for practical insulation design of the superconducting electric power apparatus [5–7].

It is well known that the area and the volume effects in SF_6 gas or transformer oil have to be included in practical designs of electrical insulation; the breakdown strength decreases with increasing the electrode area and the liquid volume subjected to high electric fields [8–11]. On the other hand, such an attempt has scarcely been made on the insulation design for superconducting devices using LN_2. In LN_2, thermal bubbles are likely to appear by thermal invasion from the room temperature environment. Some other substances such as water ice are also considered to be contaminants in LN_2. These impurities may be regarded as main weak points for the volume effect on the breakdown strength in LN_2. Moreover, micro protrusions on the electrode surface could influence the breakdown strength as weak points for the area effect, as in the case of SF_6 gas. From this point of view, we have been investigating the area and the volume effects on electrical breakdown in LN_2 in order to obtain data available for designing electrical insulation for superconducting power apparatus.

Up to the present, we have found that the area and the volume effects on breakdown voltage in LN_2 exist, and also verified quantitatively that the breakdown strength decreased with increasing $\overline{\{SEA\}}_{90}$ (90% stressed electrode area) and $\overline{\{SLV\}}_{90}$ (90% stressed liquid volume). In the present paper, we carried out statistical analysis of the experimental results using the Weibull distribution to look into the area and the volume effects on breakdown strength in LN_2.

2. STATISTICAL ANALYSIS OF BREAKDOWN STRENGTH USING WEIBULL DISTRIBUTION

As will be shown later, we employ the Weibull distribution to perform the statistical analysis for the area and the volume effects on breakdown strength in LN_2 under quasi-uniform electric field distribution. We begin with the volume effect. The weakest-link theory gives the breakdown probability p for the Weibull distribution as expressed in the form of Equation (1), (for the detail derivation, see Appendix)

$$p = 1 - \exp\left[-\frac{v}{v_0}\left(\frac{E_m}{E_0}\right)^m\right] \tag{1}$$

where m is the shape parameter, E_0 is the scale parameter, E_m is the applied maximum electric field. v/v_0 represents the number of weak points in the liquid volume; v is given by

$$v = \iiint\limits_v \left[\frac{E_i}{E_m}\right]^m dv \tag{2}$$

where E_i is a field strength at a volume unit i. Let us suppose that the volume units are small enough for E_i at the individual unit to be regarded as constant. Let v be defined as statistical stressed liquid volume (SSLV) with the relative breakdown probability $P_r = (E_i/E_m)^m$ at each unit considered. From Equation (1), the average breakdown strength E_b is obtained as given by

$$E_b = \int_0^\infty E_m \frac{dp}{dE_m} dE_m = E_0 \Gamma\left(\frac{1}{m}+1\right)\left[\frac{v}{v_0}\right]^{-1/m} \tag{3}$$

where $\Gamma(x)$ is the gamma function.

For the area effect, let us introduce statistical stressed electrode area (SSEA) S as

$$S = \iint\limits_s \left[\frac{E_i}{E_m}\right]^m dS \tag{4}$$

In this case, one can readily obtain E_b as follows

$$E_b = E_0 \Gamma\left(\frac{1}{m}+1\right)\left[\frac{S}{S_0}\right]^{-1/m} \tag{5}$$

where S/S_0 represents the number of weak points on the electrode surface. We will discuss experimental results using Equation (1) to (5).

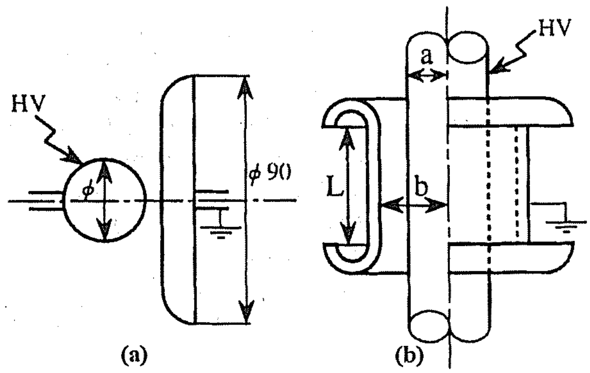

Figure 1.

Electrode configurations for breakdown voltage measurement. (a) Sphere to plane electrode (SP electrode). Diameter ϕ = 50, 20, 10, 6 mm. Gap length g = 0.5, 1.0, 1.5 mm. Surface treatment: mirror, rough. (b) Coaxial cylindrical electrode (CC electrode). Inner cylinder radius: a = 22.5, 21.5, 19.0 mm. Outer cylinder radius: b = 23.5 mm. Gap length: g = 1.0, 2.0, 4.5 mm. Effective electrode length: L = 30, 100, 350 mm. Surface treatment: mirror.

3. EXPERIMENTAL

Figures 1(a) and (b) show electrode configurations employed for breakdown voltage measurement in LN_2; sphere to plane electrode (SP electrode) and coaxial cylindrical electrode (CC electrode). All electrodes were made of stainless steel. For the SP configuration, the stressed electrode area and liquid volume varied with the sphere diameter and the gap length. The surface of the sphere electrode was made either to a mirror finish (roughness < 1 μm) or to a rough finish (roughness ~ 70 μm). On the other hand, for the CC configuration, the highly stressed electrode area and liquid volume varied with the gap length and the effective electrode length L. The gap lengths were set for three values of inner cylinder radius a. The cylindrical electrode surface was made to a mirror finish. These electrode configurations allowed the highly stressed electrode area and liquid volume to be varied from 10^0 to 10^5 mm^2 and from 10^{-1} to 10^5 mm^3, respectively as will be shown later. Thus, we can investigate the area and the volume effects in LN_2 over a wide range of the electrode size.

The SP and CC electrodes were placed horizontally and vertically in an FRP dewar, respectively, as shown in Figure 1 and immersed in LN_2. HV was applied to the sphere or to the inner cylindrical electrode. The applied voltage was either a positive or negative dc ramp voltage, or a 60 Hz ac ramp voltage at a rate of 5 kV/s. Under these conditions, we measured breakdown voltages 50 times for each experimental setup.

4. RESULTS AND DISCUSSIONS

4.1. WEIBULL PLOTS OF BREAKDOWN VOLTAGE IN LN_2

Figures 2(a) and (b) show Weibull plots of ac breakdown voltage in LN_2 with SP and CC electrodes, respectively. It is obvious from Figure 2 that the Weibull plots of ac breakdown voltage give straight lines. Another experiments for positive and negative dc voltage applications revealed that the Weibull plots of breakdown voltage were also regarded to be straight. The above results indicate that the Weibull distribution can be applied to breakdown voltages in LN_2.

Table 1 lists Weibull scale parameter E_0 and shape parameter m estimated from the slope of Weibull plots for each experimental condition. It is seen from this Table that the scale parameter E_0 for the SP configuration decreased from 86 to 113 kV/mm of the mirror finish to 76 to 97 kV/mm when the electrode surface treatment was made to a rough finish, especially for negative dc voltages. At the same time, the shape parameter m of the rough finish ($m = 7$ to 8) is a little bit larger than that of the mirror finish ($m = 6$ to 7); in other words, the scattering of the breakdown voltage for the rough finish electrode is smaller than that for the mirror finish. These results mean that making the electrode surface rough increases the number of weak points on the electrode surface, and thereby reduces E_0 and the breakdown data scatter.

On the other hand, E_0 for the CC configuration is even smaller than that for the SP configuration. The shape parameter m for CC configuration is 11 to 13, being larger than 6 to 7 for SP; the scattering of the breakdown voltage for CC is smaller than that for SP. Because the CC configuration provides much larger SSEA and SSLV than the SP configuration, it increases the number of weak points and thus the breakdown probability, resulting in the reduction of the scale parameter E_0 and the breakdown scattering as well.

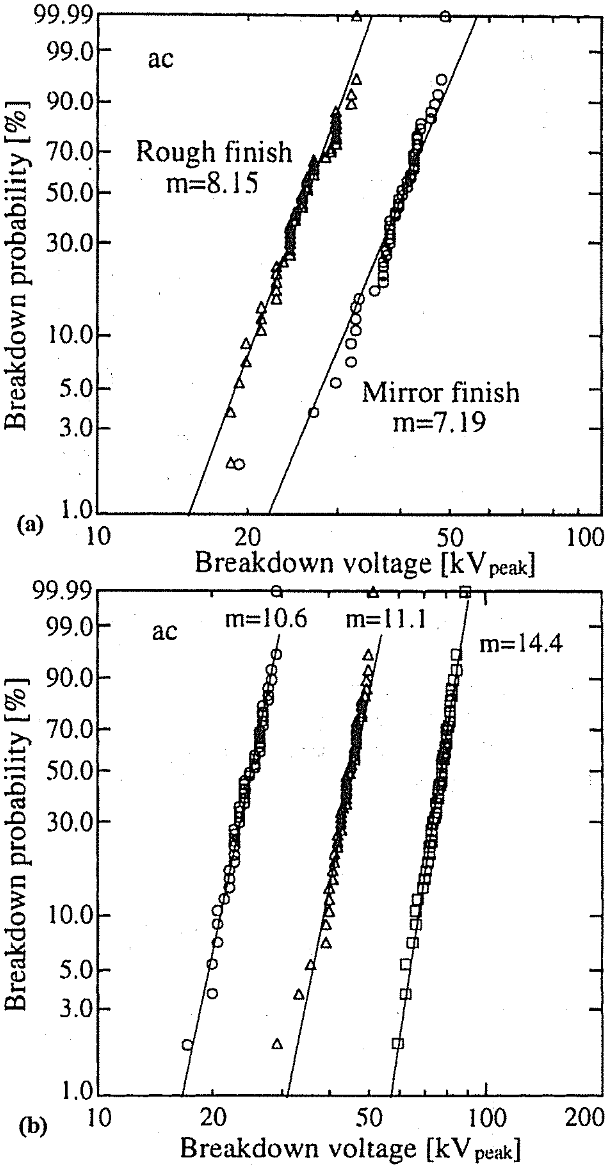

Figure 2.

Weibull plots of ac breakdown voltage in LN_2. (a) SP electrode ($\phi = 50$ mm, $g = 0.5$ mm). (b) CC electrode ($L = 100$ mm). Gap length: ○ 1.0 mm, △: 2.0 mm, □: 4.5 mm.

Table 1.
Weibull scale parameter E_0 (kV/m) and shape parameter m estimated from measured data under various conditions.

Configuration:		SP		CC
	Finish:	mirror	rough	mirror
dc+	m	7.02	7.70	11.3
	E_0	112.5	97.4	17.0
dc−	m	6.14	8.22	11.7
	E_0	100.5	79.0	17.2
ac	m	7.11	7.92	13.0
	E_0	86.3	75.8	17.8

4.2. AREA AND VOLUME EFFECTS ON BREAKDOWN STRENGTH IN LN_2

4.2.1. CALCULATION OF SSEA AND SSLV

We discussed in Section 2 the area and the volume effects on breakdown strength in LN_2 using the shape parameter m in Weibull statistics and SSEA or SSLV. Since one can obtain the electric field distribution analytically for the CC configuration, SSEA and SSLV are derived readily from Equations (2)and (4) as given in (6) and (7), respectively; (see Equations (16) and (17) in the Appendix)

$$S = 2\pi a L \left[1 + \left(\frac{a}{b}\right)^{m-1}\right] \tag{6}$$

$$\nu = \frac{2\pi}{m-2} a^2 L \left[1 - \left(\frac{a}{b}\right)^{m-2}\right] \tag{7}$$

where a and b are the inner and the outer cylinder radii, respectively, and L is the effective electrode length.

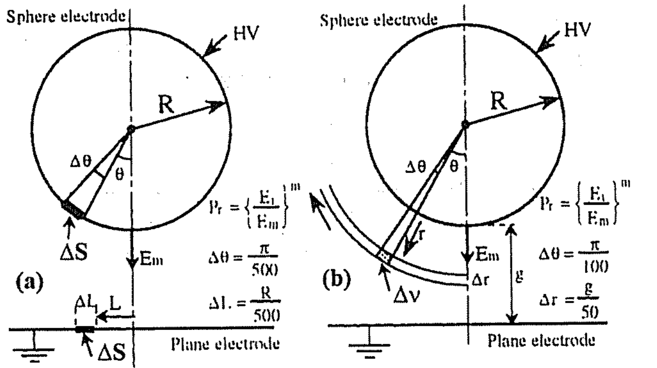

Figure 3.
Calculating methods of SSEA and SSLV for SP electrode. (a) SSEA, (b) SSLV.

On the other hand, for SP configuration it is necessary to calculate numerically SSEA and SSLV, because the electric field distribution can not be solved analytically. Hence, we calculated SSEA and SSLV for the SP configuration by the following method. Figures 3(a) and (b) show calculating methods of SSEA and SSLV, respectively for the SP electrodes. For SSEA calculation, firstly, the sphere and the plane electrode surfaces are divided into small area units. Electric field E_i at each unit is calculated by means of the charge simulation method [12]. SSEA is estimated by integrating the area unit multiplied by the relative breakdown probability P_r over the whole electrode area. For SSLV calculation, the gap space is divided into small volume units. Integration of the volume unit times P_r over the whole volume leads to SSLV. Thus calculated SSEA and SSLV allow the investigation of the statistical nature of the area and the volume effects on breakdown strength in LN_2.

4.2.2. POSITIVE dc BREAKDOWN

Figures 4(a), (b) show positive dc breakdown strength E_{B+} as a function of SSEA and SSLV, respectively. In these Figures, solid and dotted lines indicate the calculated results from Equation (3) or (5) and measured results fitted by the least squares method, respectively. It is clear that E_{B+} in LN_2 decreased to 1/5 with increasing SSEA and SSLV over the wide range from 10^0 to 10^5 mm^2 and from 10^{-1} to 10^5 mm^3, respectively. It is also evident from these Figures that the slopes of the measured lines (dotted lines) with SP electrodes are sharper than those with CC electrodes. In other words, the decrease in breakdown strength tends to saturate as SSEA and SSLV increase. These results show the appearance of the area and the volume effects on E_{B+} in LN_2. Moreover, for SP electrodes, the rough finished treatment on the sphere electrode surface causes E_{B+} to decrease a little, but keeps the slope of the measured line unchanged; the roughness on the electrode surface has little influence on the positive dc breakdown strength in LN_2.

Next, we compare the slopes of the calculated lines with those of the measured ones. For SP electrodes, the slopes of the measured lines (dotted lines) are sharper than those of calculated lines (solid lines). The discrepancy is interpreted in terms of charge injection. Further discussion about this difference in the slope will be given in Section 4.2.5.

On the other hand, for CC electrodes, the calculated values relatively agree with the measured ones. This difference from SP electrodes can be interpreted in terms of the electric field distribution. The electric field distribution for CC electrodes is more uniform in comparison with that for SP electrodes. In this case, it is considered that the charge injection effect does not effect the breakdown strength.

4.2.3. NEGATIVE dc BREAKDOWN

Figures 5(a) and (b) show the area and the volume effects on negative dc breakdown strength E_{B-} in LN_2,

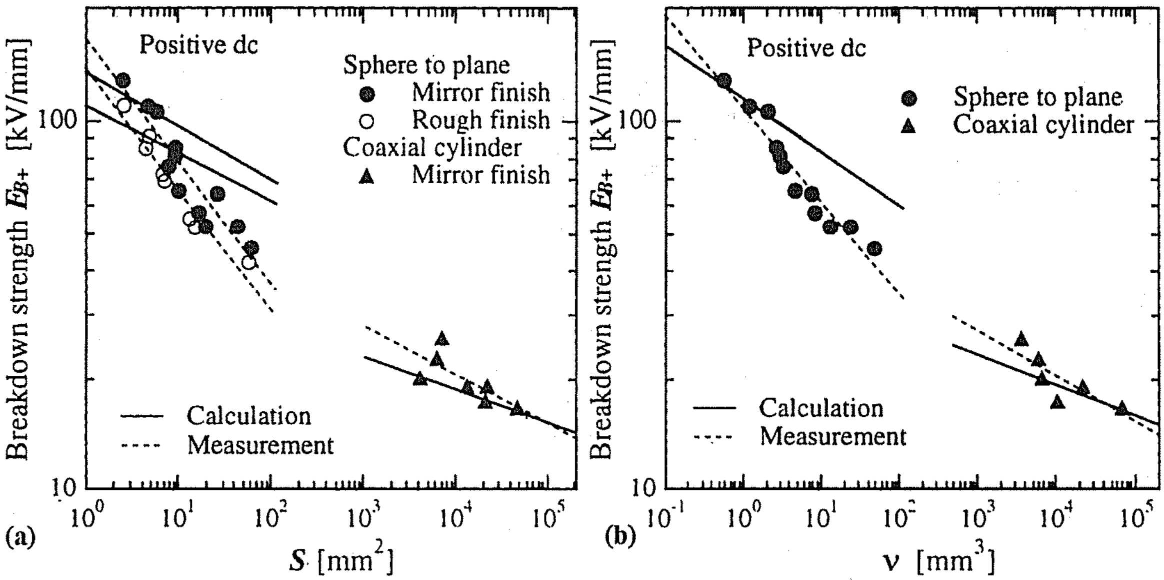

Figure 4.
Positive dc breakdown strength E_{B+} as a function of SSEA (S) and SSLV (ν). (a) Area effect. (b) Volume effect.

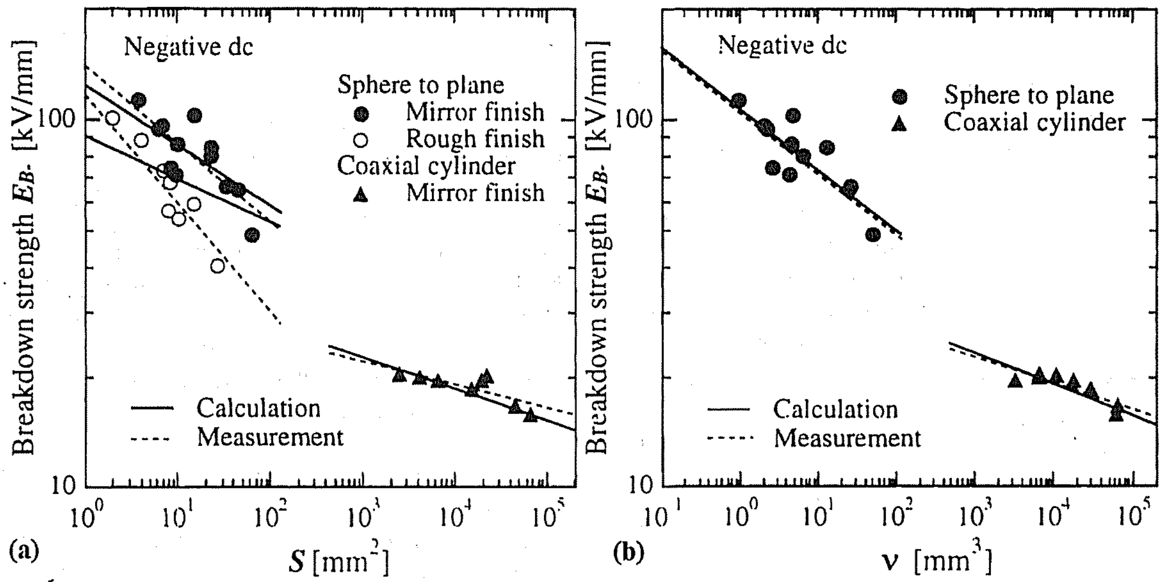

Figure 5.
Negative dc breakdown strength E_B as a function of SSEA (S) and SSLV (ν). (a) Area effect. (b) Volume effect.

respectively. As seen from the Figures, E_{B-} saturates with increasing SSEA and SSLV, as in the positive dc case. There is good agreement between the calculation and the measurement for both SP and CC electrodes with mirror finish surface treatment. However, for SP electrodes with rough finish, the slope of the measured line is steeper than that of the calculated line.

We interpret these results as follows. For negative dc voltage application to the sphere electrode, the electric field strength near the sphere cathode is enhanced. In this case, the breakdown is governed by the charge injection from the sphere cathode. Thus, if the sphere electrode surface is made rough, E_{B-} decreases by the charge injection effect as well as the area effect with increasing SSEA. The effect of the rough surface increases the size of the highly stressed electrode area, which should be included in the calculation of SSEA. This may give rise to the difference in the slope between calculation and measurement for SP electrodes with rough finish as shown in Figure 5(a). On the other hand, for the CC configuration, the slope of the measurement has proved to agree well with that of the calculation, as does the positive dc voltage case.

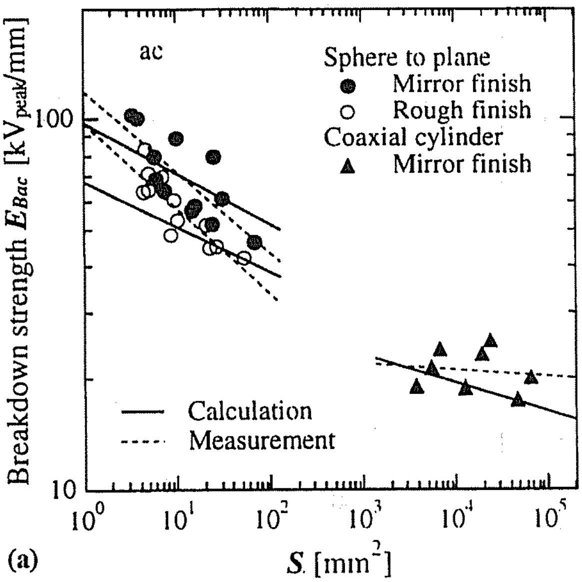

(a)

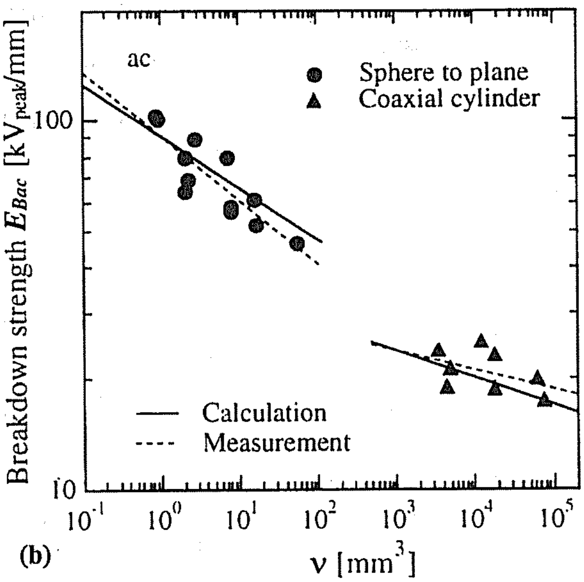

(b)

Figure 6.
ac breakdown strength E_{Bac} as a function of SSEA (S) and SSLV (ν). (a) Area effect. (b) Volume effect.

4.2.4. ac BREAKDOWN

The area and volume effects on ac breakdown strength E_{Bac} in LN_2 are shown in Figures 6(a) and (b), respectively. Note that E_{Bac} is designated as its peak value. The reduction and the saturation of the ac breakdown strength E_{Bac} with increasing SSEA and SSLV is also found as in the dc case. The calculated E_{Bac} agrees relatively well with the measurement. The reason is that the charge injection may be negligible for ac breakdown, while the area and volume effects are dominant.

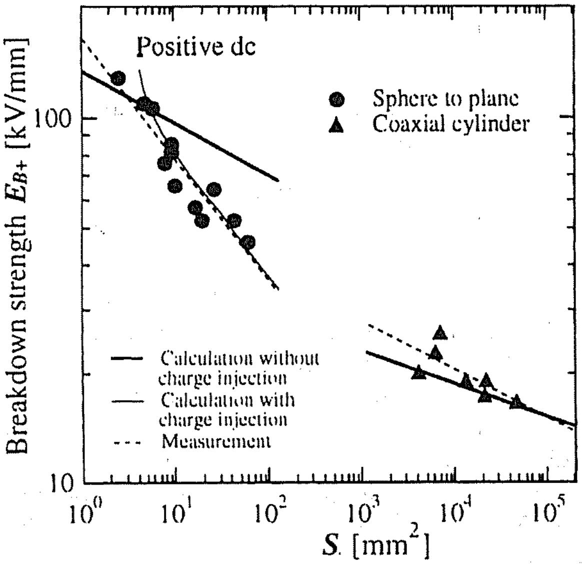

Figure 7.
Positive dc breakdown strength E_{B+} as a function of SSEA (S) with charge injection in the calculation.

4.2.5. CHARGE INJECTION EFFECT ON POSITIVE dc BREAKDOWN

As we have mentioned in Section 4.2.2, for SP electrodes, the slopes of the measured lines (dotted lines) are steeper than those of the calculated lines (solid lines) in Figure 4(a). We interpret this discrepancy of the slope in terms of the decrease in nonuniformity of the electric field distribution with increasing sphere diameter of the electrode. In the case of dc voltage, it is necessary to consider charge injection, depending on the polarity of the applied voltage. Charge injection may be considered as a kind of area effect when electrons are injected from the cathode surface. A positive dc voltage application to the sphere anode allows electrons to be injected from the opposite plane cathode. Injected electrons migrate toward the HV sphere anode, and enhance the electric field near the sphere electrode, further influencing the anode surface activities which are related to breakdown. Whereas for negative dc voltage, electrons injected from the sphere cathode enhance the electric field near the plane anode. However, this is irrelevant to breakdown near the HV sphere electrode. With these things considered, the present study assumes that the charge injection from the plane cathode affects the breakdown strength for positive dc voltage on the sphere electrode. Note that the charge injection effect from the plane cathode is ruled out in the calculation of Equation (5). When the charge injection effect is taken into account, the number of weak points should be modified by S_E, the SSEA on the plane cathode. Let us assume that, as the first approximation, the number of weak points are multiplied by electrons in the gap space and that the number of the electrons is proportional to that of the electrons injected from the plane cathode, and this number of injected electrons is proportional to S_E. In this case, Equation (5) can be replaced with Equation (8) by taking into account the increase of weak points due to the charge injection.

$$E_b = E_0 \Gamma \left(\frac{1}{m} + 1 \right) \left[\frac{S}{S_0} \frac{S_E}{S_{E_0}} \right]^{-1/m} \quad (8)$$

where S_0 and S_{E_0} represent the reference value of SSEA (S) and S_E, respectively. Figure 7 shows E_{B+} modified by Equation (8) as a function of SSEA. Thick and thin solid lines represent the plot calculated without and with the charge injection, respectively. Dotted lines represent the least squared fit of measured data. It is found that the calculated curve involving the charge injection effect agrees well with the measurement. Consequently, it is verified that charge injection has to be taken into consideration in the breakdown strength in LN_2 with SP electrodes for positive dc voltage.

4.3. RELATION BETWEEN SHAPE PARAMETER AND STRESSED ELECTRODE AREA OR LIQUID VOLUME

As shown in Equations (2) and (4), SSEA and SSLV were calculated by integrating the area and volume unit multiplied by the relative breakdown probability $P_r = (E_i/E_m)^m$ over the whole area and volume, respectively. S and v depend on the shape parameter m for the same electrode configuration. Furthermore, it is not easy in general to calculate numerically SSEA and SSLV. Therefore, for designing electrical insulation in transformer oil or SF_6 gas, 90% stressed electrode area $\{SEA\}_{90}$ and liquid volume $\{SLV\}_{90}$ to a maximum electric field E_{max} have been conventionally used [8–11]. However, it is uncertain whether $\{SEA\}_{90}$ or $\{SLV\}_{90}$ can be also used in LN_2. From this viewpoint, we examined how much percentage of E_{max} should be considered for SP electrodes using the concept of SSEA or SSLV.

Figures 8(a) and (b) show the highly stressed electrode area and liquid volume as a function of the sphere diameter for different values of $\{SEA\}_\eta$ and $\{SLV\}_\eta$ for ac voltage and mirror finished electrode surface with the gap length 1.5 mm; $\{SEA\}_\eta$ and $\{SLV\}_\eta$, respectively, indicate the electrode area and the liquid volume where the electric field exceeds η% of E_{max}. In these Figures, the shape parameter m used for SSEA and SSLV calculation comes from the measured data for ac voltage application. Note that as a value of η, 90, 85 and 80% are chosen in the Figures. It is obvious that when lies between 80 and 85%, the best fit of the calculated curve to the experimental result is obtained. In other words, SSEA or SSLV proved to correspond to 80 to 85% of SEA or SLV. This result indicates that at least 80 to 85% of E_{max} should be considered for the insulation design in LN_2 when the area and the volume effects are taken into account. These percentages are smaller by 5 to 10% than those in transformer oil and SF_6 gas [8–11]. This is due to the fact that the breakdown voltage in LN_2 scatters much more than those in transformer oil and SF_6 gas due to the presence of thermal bubbles which may cause an increase in weak points, *etc.* Note that these percentages depend on various factors such as gap length, electrode configuration, electrode surface treatment, pressure, and so on.

As mentioned above, we examined breakdown characteristics in LN_2 from the aspect of both area and volume effects. In LN_2, small bubbles are likely to appear, and thus may contribute to the volume effect. Moreover, by studying the area effect for the rough finish surface treatment, it can be said that the area effect may be significant.

Thus, not only the volume effect but also the area effect, having a mutual correlation, simultaneously may cause the degradation of breakdown strength in LN_2. In this work, it is not essential to separate the contribution of the area and the volume effects on breakdown voltage in LN_2. Concerning the issue, further investigation is in progress and will be published in the future.

5. CONCLUSION

WE measured breakdown voltage in LN_2 with the sphere to plane electrode (SP electrodes) and the coaxial cylindrical electrode (CC electrodes). We also performed Weibull statistical analysis of the experimental results to investigate area and volume effects on breakdown strength in LN_2. These electrode configurations allowed SSEA and SSLV to be widely varied over 5 to 6 orders of the size from 10^0 to 10^5 mm^2 and from 10^{-1} to 10^5 mm^3, respectively. The results are summarized as follows.

The dc and ac breakdown strength in LN_2 decreased to 1/5 with increasing the SSEA and the SSLV. The Weibull shape parameter m of the rough finish electrode surface treatment ($m = 7$ to 8) was larger than that of the mirror finish ($m = 6$ to 7) for SP electrodes. Thus, the scattering of the breakdown voltage for the rough finish was smaller than that of the mirror finish. This result indicated that making the electrode surface rough increased the number of weak points on the electrode surface and reduced the breakdown voltage and scattering. On the other hand, the shape parameter m for CC electrodes was estimated to be 11 to 13, being larger than those for SP electrodes. Thus, the breakdown strength saturated

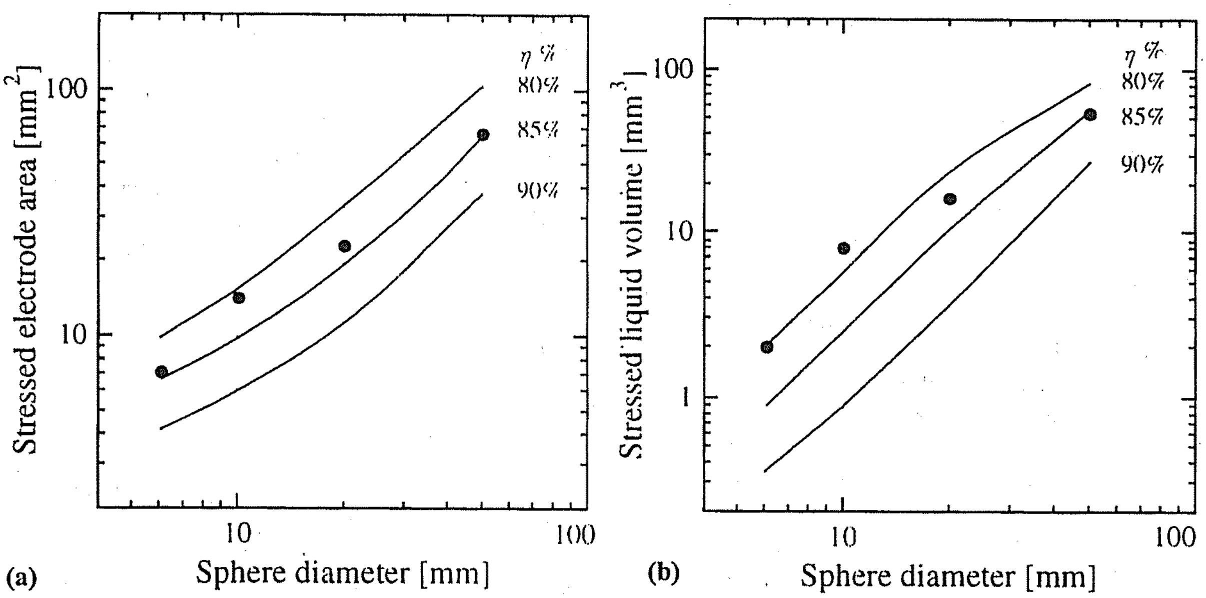

Figure 8.

Highly stressed electrode area and liquid volume as a function of sphere diameter for different value of η. η represents the percentage of E_{max} to be considered for SEA and SLV calculation. (ac, mirror finish, gap length: 1.5 mm) (a) Stressed electrode area. (b) Stressed liquid volume.

with increasing SSEA and SSLV. These results permitted us to confirm that the area and the volume effects definitely determined the breakdown strength in LN_2.

The measured negative dc and ac breakdown strength agreed relatively well with the calculation from Weibull statistical analysis for both SP and CC electrodes. Whereas for positive dc voltage on the sphere electrode, it was suggested that the breakdown strength was governed by the charge injection effect from the plane cathode. For this case, a modification of the calculation was made with the charge injection effect considered. Consequently, the modified values agreed well with the measured ones.

SSEA or SSLV was found to correspond to 80 to 85% SEA or SLV. This result indicated that at least 80 to 85% of the maximum electric field strength should be considered for insulation design of the apparatus in LN_2 when the area and the volume effects are taken into account.

APPENDIX

As shown in Section 2, we employed the Weibull distribution to carry out the statistical analysis for the area and the volume effects on breakdown strength in LN_2. In this Appendix, we show how to derive the statistical equations for the quasi-uniform field using the Weibull distribution in detail.

We begin with the volume effect. Suppose that the gap space is divided into n pieces of small volume units, and that p_i is the breakdown probability of each unit i. In this case, let us suppose that volume units are small enough for the electric field strength at the individual unit to be regarded as constant. Then, the weakest-link theory gives the whole breakdown probability p as expressed by

$$\ln(1-p) = \sum_{i=1}^{n} \ln(1-p_i) \tag{9}$$

If E_i is the electric field at the unit i, Weibull statistics permit p_i to be given by

$$\ln(1-p_i) = \left[\frac{E_i}{E_0}\right]^m \tag{10}$$

where m is the shape parameter, and E_0 is the scale parameter. We rearrange Equation (9) by substituting Equation (10) as expressed by

$$\begin{aligned}\ln(1-p) &= \sum_{i=1}^{v} \left[\frac{E_i}{E_0}\right]^m \\ &= \frac{1}{v_0}\iiint_v \left[\frac{E_i}{E_0}\right]^m dv \\ &= \frac{1}{v_0}\iiint_v \left[\frac{E_i}{E_m}\right]^m dv \left[\frac{E_m}{E_0}\right]^m \\ &= \frac{v}{v_0}\left[\frac{E_m}{E_0}\right]^m\end{aligned} \tag{11}$$

where E_m is the maximum electric field, v_0 represents the reference value of the liquid volume, and v is defined as statistical stressed liquid volume (SSLV) as given by Equation (2).

Thus, SSLV is the statistical stressed liquid volume taking into account the relative breakdown probability $P_r = (E_i/E_m)^m$ at the unit i. v/v_0 corresponds to the number of weak points.

Equation (11) gives the whole breakdown probability p for the Weibull distribution as expressed by

$$p = 1 - \exp\left[-\frac{v}{v_0}\left(\frac{E_m}{E_0}\right)^m\right] \tag{12}$$

From Equation (12), the average breakdown strength E_b is obtained as given by

$$\begin{aligned} E_b &= \int_0^\infty E_m \left[\frac{dp}{dE_m}\right] dE_m \\ &= \int_0^\infty m\frac{v}{v_0}\left[\frac{E_m}{E_0}\right]^m \exp\left[-\frac{v}{v_0}\left(\frac{E_m}{E_0}\right)^m\right] dE_m \qquad (13) \\ &= E_0 \Gamma\left(\frac{1}{m}+1\right)\left[\frac{v}{v_0}\right]^{-1/m} \end{aligned}$$

For example, for a coaxial cylindrical electrode configuration, E_i is obtained analytically as given by

$$E_i = \frac{V}{r\ln(b/a)} = \frac{a}{r}E_m \tag{14}$$

where a and b are the inner and the outer cylinder radii, respectively, r is the radius at the unit i, and V is the applied voltage. From Equation (14), P_r is given by

$$P_r = \left[\frac{a}{r}\right]^m \tag{15}$$

From Equations (2) and (15), SSLV for the coaxial cylindrical electrode is given by

$$\begin{aligned} v &= \int_a^b \left[\frac{a}{r}\right]^m 2\pi r L\, dr \\ &= \left[\frac{2\pi}{m-2}\right] a^2 L \left[1 - \left(\frac{a}{b}\right)^{m-2}\right] \end{aligned} \tag{16}$$

where L is the effective electrode length.

For the area effect, let us use the statistical stressed electrode area (SSEA) as defined in Equation (4), In this case, one can readily obtain E_b as given in Equation (5).

For instance, SSEA for the coaxial cylindrical electrode is given by Equation (17) as SSLV does,

$$\begin{aligned} S &= \int_0^{2\pi} La d\theta + \int_0^{2\pi} \left(\frac{a}{b}\right)^m Lb\, d\theta \\ &= 2\pi a L\left[1 + \left(\frac{a}{b}\right)^{m-1}\right] \end{aligned} \tag{17}$$

REFERENCES

[1] H. Fujino, "Electrical Insulation Technology for Superconducting Devices in Japan", IEEE Electrical Insulation Magazine, Vol. 6, No. 2, pp. 7–15, 1990.

[2] M. Hara, T. Kaneko and K. Honda, "Electrical Breakdown Mechanism of Liquid Nitrogen in the Presence of Thermally Induced Bubbles", Cryogenics, Vol. 27, pp. 93–101, 1987.

[3] M. Hara, H. Koishihara and K. Saita, "Breakdown Behavior of Cryogenic Liquids in the Presence of Thermal Bubble under Ramped Voltage", IEEE Trans. EI, Vol. 26, No. 4, pp. 685–691, 1991.

[4] R. J. Meats, "The Impulse Voltage Flashover of Dielectric Spacers in a Helium-insulated Superconducting Cable Model", Cryogenics, Vol. 27, pp. 77–80, 1977.

[5] J. Gerhold, "Electrical Insulation in Superconducting Power Systems", IEEE Electrical Insulation Magazine, Vol. 8, No. 3, pp. 14–20, 1992.

[6] J. Gerhold and M. Hara, "Procedure of Electrical Insulation Design for Superconducting Coils", Proc. of 8th ISH, 93.04, pp. 567–570, 1993.

[7] H. Goshima, T. Suzuki, N. Hayakawa, M. Hikita and H. Okubo, "Dielectric Breakdown Characteristics of Cryogenic Nitrogen Gas above Liquid Nitrogen", IEEE Trans. Dielectrics and EI, Vol. 1, No. 3, pp. 538–543, 1994.

[8] P. J. Sinz, *Influence of Moisture and Particles on the Electric Strength of Insulating Oils*, Doctor thesis of the Technical University of Graz, 1990.

[9] Y. Kawaguchi, H. Murata and M. Ikeda, "Breakdown of Transformer Oil", IEEE Trans. PAS, Vol. 91, No. 1, pp. 9–23, 1972.

[10] M. Ikeda, T. Teranishi, M. Honda and T. Yanari, "Breakdown Characteristics of Moving Transformer Oil", IEEE Trans. PAS, Vol. 100, No. 2, pp. 921–928, 1981.

[11] A. Rein and J. Kulstas, "Impulse Breakdown of SF_6/N_2 Insulation. Influence of Electrode Covering. Polarity Effects", *Gaseous Dielectrics* III, pp. 315–320, 1982.

[12] H. Singer, H. Steinbigler and P. Weiß, "A Charge Simulation Method for the Calculation of High Voltage Fields", IEEE Trans. PAS, Vol. 93, No. 5, pp. 1660–1668, 1974.

Manuscript was received on 19 July 1994, in revised form 5 January 1995.